NiFe Hydrogenase Active Site Biosynthesis: Identification of Hyp Protein Complexes in *Ralstonia eutropha*†

Anne K. Jones, Oliver Lenz, Angelika Strack, Thorsten Buhrke, and Bärbel Friedrich*

Institut für Biologie, Humboldt-Universität zu Berlin, 10115 Berlin, Germany

Received June 7, 2004; Revised Manuscript Received July 30, 2004

ABSTRACT: Biosynthesis of the NiFe hydrogenase active site is a complex process involving the action of the Hyp proteins: HypA−HypF. Here we investigate the mechanism of NiFe site biosynthesis in *Ralstonia eutropha* by examining the interactions between HypC, HypD, HypE, and HypF1. Using an affinity purification procedure based on the *Strep*-tag II, we purified HypC and HypE from different genetic backgrounds as complexes with other hydrogenase-related proteins and characterized them using immunological analysis. Copurification of HypC and HoxH, the active site-containing subunit of the soluble hydrogenase in *R. eutropha*, from several different genetic backgrounds suggests that this complex forms early in the maturation process. With respect to the Hyp proteins, it is shown that HypE and HypF1 formed a stable complex both in vivo and in vitro. Furthermore, HypC and HypD functioned as a unit. Together, they were able to interact with HypE to form a range of complexes probably varying in stoichiometry. The HypC/HypD/HypE complexes did not involve HypF1 but appeared to be more stable when HypF1 was also present in the cells. We hypothesize that HypF1 is able to modify some component of the HypC/HypD/HypE complex. Since we have also seen that HypF1 and HypE form a complex, it is likely that HypF1 modifies HypE. On the basis of these results, we propose a complete catalytic cycle for HypE. First, it is modified by HypF1, and then it can form a complex with HypC/HypD. This activated HypE/HypC/HypD complex could then decompose by donating active site components to the immature hydrogenase and regenerate unmodified HypE.

The reversible oxidation of hydrogen, catalyzed by the enzymes known as hydrogenases, plays a crucial role in bacterial energy metabolism. Hydrogen oxidation can be used to produce reducing equivalents, or electrons can be disposed of via proton reduction. The mechanism of hydrogenase action is of interest not only to chemists and biochemists but also to engineers of hydrogen-based, energy-generation devices, and therefore many aspects of hydrogenase structure and function have been carefully scrutinized (*1*). The unusual active site architecture of hydrogenases makes their biosynthesis a particularly challenging topic. The majority of hydrogenases contain a dinuclear active site, either FeFe or NiFe, redox-linked to the surface via iron−sulfur clusters (*2*−*8*). Fourier transform infrared (FTIR) spectroscopy has shown that both the Fe−Fe bimetallic center and the Ni−Fe site contain endogenous CO and CN^- ligands coordinated to Fe, making hydrogenases the only category of enzymes to have this property. In addition, the NiFe site is completed by four conserved cysteine residues coordinating the Ni, two also bridging the Fe ion, giving an overall $(Cys)_2Ni(\mu\text{-}Cys)_2Fe(CN)_2(CO)$ structure. Elucidation of the mechanism of ligand biosynthesis and incorporation into hydrogenases is one of the most interesting mysteries facing bioinorganic chemists.

Biochemical studies, primarily using *Escherichia coli* as a model system, have led to an outline for the mechanism of NiFe active site biosynthesis. At least six accessory gene products, HypA, HypB, HypC, HypD, HypE, and HypF, are required for NiFe site biosynthesis (for a review, see ref *9*). A few organisms that produce hydrogenases under aerobic conditions also harbor an additional *hyp* gene, *hypX*, which is essential for full hydrogenase activity (*10*−*12*). In *E. coli*, HypE and HypF are proposed to function together in the synthesis of the diatomic ligands. Mass spectrometry showed that HypF utilizes carbamoyl phosphate and ATP as substrates to synthesize an enzyme−thiocarbamate at the conserved C-terminal cysteine of HypE (*13*−*15*). This S-carbamoyl moiety can then be dehydrated in another ATP-dependent reaction to yield a thiocyanate. Although no experimental evidence using the biological system has yet been obtained, based on synthetic inorganic chemistry precedents, a similar dehydration reaction has been suggested for the synthesis of CO. It is proposed that then the diatomic ligands are transferred to an Fe residing in a HypC/HypD complex. Evidence for this hypothesis comes from the accumulation of a HypC/HypD complex in *E. coli* cells deprived of carbamoyl phosphate and its resolution when the cells are supplemented with citrulline, a compound that can be metabolized to carbamoyl phosphate (*16*). Then HypC, together with the Fe fragment, is believed to be transferred from the HypC/HypD complex to the immature

† This work has been funded by the Deutsche Forschungsgemeinschaft, the Fonds der Chemischen Industrie, and SFB498 (TP C1). A.K.J. acknowledges the Alexander von Humboldt Foundation for a fellowship.

* To whom correspondence should be addressed. E-mail: baerbel.friedrich@rz.hu-berlin.de. Tel: +49-30-20938100. Fax: +49-30-20938102.

10.1021/bi048837k CCC: $27.50
Published on Web 10/02/2004

hydrogenase, a step proposed because HypC has also been observed in a complex with the immature hydrogenase large subunit (*17*−*19*). In this complex, HypC would function as a chaperone to prevent folding before incorporation of Ni through the GTP-dependent action of HypB in concert with HypA (*20*, *21*). Finally, a C-terminal extension of the hydrogenase large subunit is cleaved by a specific endopeptidase before oligomerization (*22*−*25*).

In this study, we investigate the mechanism of NiFe active site biosynthesis in *Ralstonia eutropha*, an organism that produces hydrogenases under aerobic conditions. *R. eutropha*, a facultative chemolithoautotrophic β-proteobacterium, possesses two energy-linked hydrogenases, one membrane-bound (MBH) and the other soluble (SH), as well as a hydrogen-sensing hydrogenase (RH) (*26*−*28*). The mechanism of the biosynthesis of the diatomic ligands in *R. eutropha* is of particular interest since the SH has been shown using FTIR spectroscopy to have a unique active site containing additional CN^- ligands on both the Ni and the Fe (*29*). The hydrogenase-related genes of *R. eutropha* are located on the megaplasmid pHG1 in two distinct operons (*30*). A complete set of *hyp* genes, (*hypA1B1F1CDEX*) is associated with the MBH structural and accessory genes whereas copies of three of the *hyp* genes (*hypA2B2F2*) are associated with the SH genes (*31*, *32*). HypF1 is a truncated HypF protein relative to HypF2 and HypF from *E. coli* and contains only one of the three functional domains usually present in HypF proteins. In this paper, using a *Strep*-tag II affinity purification procedure, we purified homologously produced HypE and HypC. Purification of these proteins from different genetic backgrounds has permitted isolation of several different Hyp protein complexes. These complexes demonstrate interactions between HypC/HypD and HypE, as well as providing a role for HypF1 in the maturation of hydrogenases in *R. eutropha*.

MATERIALS AND METHODS

Strains and Plasmids. The strains and plasmids used in this study are presented in Table 1. Strains with the intials HF were derived from wild-type *R. eutropha* H16. *E. coli* JM109 (*33*) was used for standard cloning procedures, and *E. coli* S17−1 (*34*) was used for conjugative plasmid transfer to *R. eutropha* strains.

Plasmids pCH1048, pCH1049, pCH1051, and pCH1053[1] were designed for plasmid-based overexpression of *hypC*, *hypE*, and *hypF1* with a *Strep*-tag II coding sequence under the control of a modified *acoX* promoter of *R. eutropha* (*35*). Each was prepared using an analogous procedure. The tags and *Nde*I and *Nco*I restriction sites for cloning were introduced by PCR amplification of the desired gene using pCH103 as the template and the appropriate primers: *hypE* with upstream tag sequence using oligonucleotides 521 and 522; *hypE* with downstream tag sequence using oligonucleotides 523 and 524; *hypC* with downstream tag sequence using oligonucleotides 525 and 526; *hypF1* with downstream tag sequence using oligonucleotides 527 and 528. The resulting fragments were cloned into *Nde*I/*Nco*I digested pLO10 producing plasmids pCH1046, pCH1047, pCH1050, and pCH1052. These pLO10-derived plasmids were then digested with *Acc*65I to yield fragments containing the gene of interest and the modified *acoX* promoter, which were then cloned into pCM62. These pCM62-derived plasmids were transferred to *R. eutropha* via conjugation.

Media and Growth Conditions. E. coli strains were grown in Luria broth (LB). *R. eutropha* strains were grown in modified LB medium containing no sodium chloride or in mineral salts medium (*39*) containing 0.4% fructose (FN) or a mixture of fructose and glycerol (0.2% [w/v] each; FGN). Solid media contained 1.5% (w/v) agar. Antibiotics were added to a final concentration of 15 μg mL^{-1} for tetracycline and 100 μg mL^{-1} for ampicillin.

Conjugative Plasmid Transfer. Mobilizable plasmids were transferred from *E. coli* to *R. eutropha* by using a spot mating technique (*34*).

Protein Purification and Immunoblot Analysis. All purification steps were carried out at 4 °C. *R. eutropha* cells were grown in FGN medium for 48 h to an OD_{436} of 11 and then harvested by centrifugation. After resuspension in 50 mM potassium phosphate buffer (pH 7), the cells were then disrupted by two passages through a chilled French pressure cell (Amicon). Cell debris and membranes were separated from the soluble fraction by ultracentrifugation for 30 min at 90 000 × *g*. The soluble extract was then applied to a 1 mL *Strep*-Tactin Superflow (IBA, Göttingen, Germany) column by gravity flow. Unbound proteins were removed by washing with three column volumes of buffer A (100 mM Tris/HCl, pH 8, 150 mM NaCl). Protein was then eluted from the column in 0.5 mL fractions using buffer B (buffer A with 5 mM desthiobiotin).

Protein concentrations were determined using the method of Bradford (*40*) using bovine serum albumin as a standard.

Antibodies directed against the Hyp proteins were obtained using the following protocol: N-terminal His-tag fusions of the respective *R. eutropha* Hyp proteins were heterologously overproduced in *E. coli* and purified via Ni−NTA affinity chromatography under denaturing conditions. The purified proteins were then used for rabbit immunization. In the case of HoxH antibody production, native SH was purified from *R. eutropha* using a standard protocol, and the SH subunits were subsequently separated by preparative SDS−PAGE (*41*).

For immunoblot analysis, proteins were separated in polyacrylamide gels (PAGE) (*42*) and transferred to nitrocellulose membranes (Biotrace NT, Pall, Michigan) according to a standard protocol (*43*). Proteins were detected with antibodies raised against HoxH (1:25 000), HypB1 (1:2000), HypC (1:500), HypD (1:1000), HypE (1:500), HypF1 (1:5000), or HypX (1:500) and alkaline phosphatase-labeled goat anti-rabbit immunoglobulin G (Dianova, Hamburg, Germany). *Strep*-tag II monoclonal antibodies were obtained from IBA (Göttingen, Germany) and used as directed by the manufacturer with goat anti-mouse antibody (Bio-Rad). Molecular weight marker for use under nondenaturing conditions was obtained from Gradipore (Australia).

Molecular Mass Determination by Native Gel Electrophoresis. The procedure described by Spinelli et al. (*44*) as modified from Hedrick and Smith (*45*) was used. Two microliters of 1 mg mL^{-1} protein solutions were subjected

[1] Abbreviations: Plasmids will be referred to using the following descriptive nomenclature. A pCM62-derived plasmid carrying P_{Aco} and *geneX* producing a protein with a C-terminal *Strep*-tag II tag will be referred to as p*geneX*$_{SC}$. Similarly, an N-terminal tag will be indicated as p*geneX*$_{SN}$.

Table 1: Strains, Plasmids, and Oligonucleotides Used in This Study

strain, plasmid or oligonucleotide[a]	relevant characteristics or sequence[b]	source or ref
R. eutropha		
H16	wild-type, SH^+, MBH^+, RH^+, $HoxJ^-$ (*hoxJ*g1264a)	DSM428, ATCC 17699
HF210	pHG1Δ	*36*
HF338	*hypD*Δ, $HoxJ^-$	*31*
HF339	*hypE*Δ, $HoxJ^-$	*31*
HF340	*hypC*Δ, $HoxJ^-$	*31*
HF417	*hypB1*Δ, *hypB2*Δ, $HoxJ^-$	*32*
HF441	*hypF1*Δ, *hypF2*Δ, $HoxJ^-$	*32*
E. coli		
JM109	F′, *tra*D36, *lac*I^qΔ(*lac*Z)M15 *pro*A^+B^+/e14^- ($McrA^-$), Δ(*lac-pro*AB), *thi*, *gyrA96* (Nal^r), *endA1*, *hsd*R17(r_K-m_K^+), *rel*A1, *supE44*, *recA1*	*33*
S17-1	Tra^+, *recA*, *pro*, *thi*, *hsdR*, *chr*::RP4-2	*34*
Plasmids		
pCM62	RK2*ori*, ColE1*ori*, Tc^r, Mob^+, P_{lac}, *lacZ*	*37*
pLO10	ColE1*ori*, P_{lac}, P_{acoX}, SD_{hoxF}, Ap^r	Lenz and Friedrich
pCH103	pSUP202 with an 8.3 kb *Eco*RI fragment containing *hypA1*−*hypX*	*38*
pCH1046	pLO10 with a 1.1 kb *Nde*I/*Nco*I fragment containing *hypE* with the *Strep*-tag II coding sequence attached upstream	this study
pCH1047	pLO10 with a 1.1 kb *Nde*I/*Nco*I fragment containing *hypE* with the *Strep*-tag II coding sequence attached downstream	this study
pCH1048 (p*hypE*$_{SN}$)	pCM62 with a 1.7 kb *Acc*65I fragment derived from pCH1046	this study
pCH1049 (p*hypE*$_{SC}$)	pCM62 with a 1.7 kb *Acc*65I fragment derived from pCH1047	this study
pCH1050	pLO10 with a 300 bp *NdeI*/*Nco*I fragment containing *hypC* with the *Strep*-tag II coding sequence attached downstream	this study
pCH1051 (p*hypC*$_{SC}$)	pCM62 with a 900 bp *Acc*65I fragment derived from pCH1050	this study
pCH1052	pLO10 with a 1.3 kb *Nde*I/*Nco*I fragment containing *hypF1* with the *Strep*-tag II coding sequence attached downstream	this study
pCH1053 (p*hypF1*$_{SC}$)	pCM62 with a 1.9 kb *Acc*65I fragment derived from pCH1052	this study
Oligonucleotides[c]		
521	GGAGCAGCAcatatgtggagccacccgcagttcgaaaaaggcgcc AGCGGCACCGTTAAACTGGGCTATCAA	this study
522	CGTAGCccatggTCAACAAATGCGCGGAAGCTGCTCGCCGGA	this study
523	GGAGCAGCAcatATGAGCGGCACCGTTAAACTGGGCTATCAA	this study
524	CGTAGCccatggtcatttttcgaactgcgggtggctccaagcgct ACAAATGCGCGGAAGCTGCTCGCCGGACAG	this study
525	GGAGGAGGGCGCGCCcatATGTGCCTAGCGATTCCCG CACGTTTGGTGGAA	this study
526	CGTAGCccatggtcatttttcgaactgcgggtggctccaagcgct TGCCGGCTCCTGATGAATGTTCATCCCATG	this study
527	GGACGTAGCcatATGCGAGCGCAGACCTTGCCAGCCGGCAGC	this study
528	CGTAGCccatggtcatttttcgaactgcgggtggctccaagcgct GGCACATGGCGCGCCCTCCTCCTGTAGATG	this study

[a] Designations in parentheses indicate descriptive names for the plasmids used in the text. [b] Ap^r, ampicillin resistant; Tc^r, tetracycline resistant. [c] New bases either for new restriction sites or the *Strep*-tag II coding sequence are indicated in lowercase letters.

to electrophoresis at 4 °C on 6 cm long gels containing 6%, 8%, 10%, and 12.5% (w/v) acrylamide. The gels were subsequently stained with Coomassie stain, and the R_f of each protein or complex was determined. A plot of 100 log(100R_f) versus acrylamide concentration resulting in a straight line was made for each protein. The slopes of these lines were then plotted against the molecular mass. The following protein standards (Sigma) were used to calculate a calibration curve: lactic dehydrogenase (36 kDa), bovine serum albumin (66 kDa), alcohol dehydrogenase from yeast (150 kDa), and β-amylase from sweet potato (200 kDa).

Hydrogenase Activity Assay. Soluble hydrogenase activity, H_2-dependent NAD^+ reduction, was determined spectrophotometrically using the soluble fraction of cells grown heterotrophically on FGN to an OD_{436} of 10 (*28*).

RESULTS

Complementation of Hydrogenase Activity. To facilitate quick purification of Hyp protein complexes from *R. eutropha*, we constructed, as described in the Materials and Methods, plasmids for the expression of single *hyp* genes fused to the *Strep*-tag II coding sequence.[1] The expression plasmids were transferred to the corresponding *hyp* deletion strains to establish by genetic complementation whether the *Strep*-tagged Hyp proteins were functionally active in *R. eutropha*. Previous work has shown that deletion of one or

more *hyp* genes in *R. eutropha* resulted in loss of hydrogenase activity (*31*, *32*, *46*). Therefore, the *Strep*-tagged proteins were assessed for their ability to restore SH activity. Transfer of plasmids p*hypC*$_{SC}$ and p*hypF1*$_{SC}$ to HF340 (*hypC*Δ) and HF441 (*hypF1F2*Δ), respectively, restored SH activity to the wild-type level. In the case of HypE, an N-terminal *Strep*-tag II fusion produced from p*hypE*$_{SN}$ was able to restore SH activity in the HypE$^-$ strain. However, the introduction of plasmid p*hypE*$_{SC}$, producing HypE fused to a *Strep*-tag II at the C-terminus, did not complement the deletion in the HypE$^-$ strain. Western blot analysis showed that both p*hypE*$_{SN}$ and p*hypE*$_{SC}$ produced HypE at similar levels (data not shown). Therefore, HypE with an N-terminally fused *Strep*-tag II was physiologically active in maturation of SH, whereas HypE with a C-terminal tag, that is, in which the conserved C-terminal cysteine residue is presumably blocked, was not.

Purification of HypE from a Wild-Type Background. Complex formation in vivo can be studied via copurification of protein complexes. Therefore, N-terminally tagged HypE was purified using an affinity procedure based on the *Strep*-tag II to establish whether other Hyp proteins were copurified (see Materials and Methods for procedure details). Figure 1A shows a Coomassie-stained SDS−polyacrylamide gel of the proteins resulting from the purification of an extract of HF339[*hypE*Δ](p*hypE*$_{SN}$) over a *Strep*-Tactin Superflow column. The majority of the protein in the elution fractions was HypE (36.6 kDa), as determined by immunoblot analysis using HypE-specific antiserum (Figure 1B). There are two non-hydrogenase-related contaminants that migrate with masses between 62 and 83 kDa. Using mass spectrometry, we have determined them to be homologues of DnaK and propionyl-CoA(S)-methyl-malonyl-CoA carboxylase (Jones, Krause, and Friedrich, unpublished results). These two proteins were also retained on the column when no *Strep*-tagged protein was present in the extract, that is, when wild-type *R. eutropha* soluble extract was applied to the column and the same washing and elution procedure was used (data not shown). In addition, several other Hyp proteins copurified with HypE. As shown in Figure 1B, immunoblot analysis using HypC- (9.8 kDa), HypD- (42 kDa), and HypF1-specific (40.7 kDa) antisera established that the other two bands present with molecular masses between 47.5 and 32.5 kDa were HypD and HypF1. Furthermore, detectable quantities of HypC were also present in the elution fractions. On the other hand, analysis showed that HypB1 and HypX were not copurified with HypE (data not shown). Using serum against the large subunit of the SH, HoxH, revealed no traces of this protein in the partially purified HypE, indicating that under these conditions HoxH is not copurified with the Hyp proteins. The retention of the various Hyp proteins on the column was not equal. Figure 1A shows that whereas HypE was only present in the elution fractions, the HypD and HypF1 bands were also observed in the last wash fraction, that is, before desthiobiotin was added to the column. This suggests that they were not as tightly bound to the column as HypE. Furthermore, they were present at much lower quantities than the HypE. This is to be expected since HypE alone was overexpressed from the plasmid whereas the other Hyp proteins were only present at unenhanced, wild-type levels. These results show that HypC, HypD, and HypF1 copurified with HypE under wild-type-like conditions and

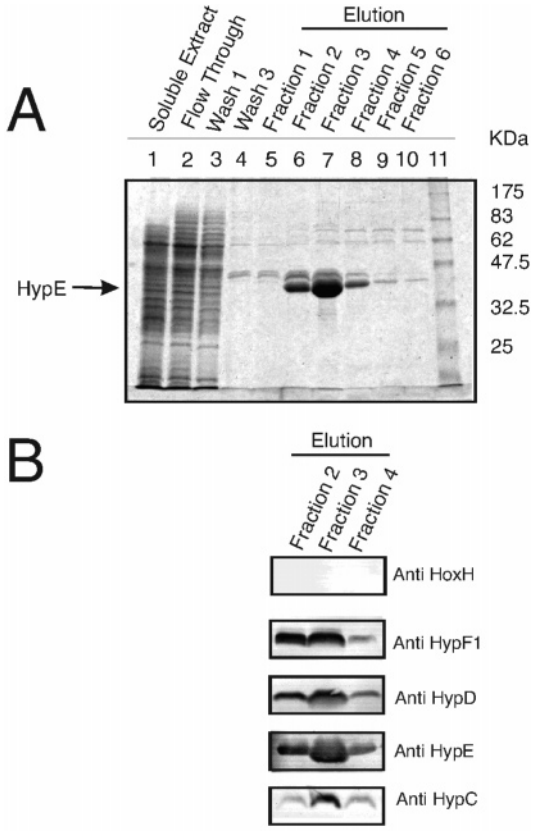

FIGURE 1: Purification of N-terminally *Strep*-tagged HypE from HF339[*hypE*Δ](p*hypE*$_{SN}$). In panel A, the indicated proteins were separated on a 12% SDS−PAGE gel and visualized with Coomassie brilliant blue: lane 1, crude soluble extract; lane 2, column flow through; lane 3, first column volume of washing buffer; lane 4, third column volume of washing buffer; lane 5, first elution fraction; lane 6, second elution fraction; lane 7, third elution fraction; lane 8, fourth elution fraction; lane 9, fifth elution fraction; lane 10, sixth elution fraction; lane 11, standard proteins. In each of lanes 4−10, 15 μL of the designated sample was applied to the gel. Panel B shows Western blot analysis of elution fractions 2, 3, and 4 using the specific antisera designated adjacently. For analysis with HoxH-, HypF1-, HypD-, and HypE-specific antisera, the proteins were separated by 12% SDS−PAGE. However, 15% SDS−PAGE was used for analysis with anti-HypC-specific serum.

demonstrate that one or more complexes, each involving HypE, must be formed.

Despite its lack of activity, to establish whether complex formation with HypE could still take place, an analogous purification of C-terminally *Strep*-tagged HypE from HF339-[*hypE*Δ](p*hypE*$_{SC}$) cells was also undertaken. Again, considerable quantities of HypE were detected in the eluted proteins. However, only traces of HypC and HypD and no HypF1 were detected in the elution fractions (data not shown). This demonstrates that masking the C-terminal cysteine of HypE with a small peptide not only led to inactivity but significantly inhibits complex formation between HypE and the other Hyp proteins.

Purification of HypE from hyp Deletion Mutants. To obtain more information with respect to the interactions between HypC, HypD, HypE, and HypF1, p*hypE*$_{SN}$ was introduced into *R. eutropha* H16-derived strains in which one of the *hyp* genes was deleted, and cell-free soluble extracts were purified over a *Strep*-Tactin Superflow column using the same procedure described above. Figure 2 shows the results of immunoblot analysis of the purified proteins. Three

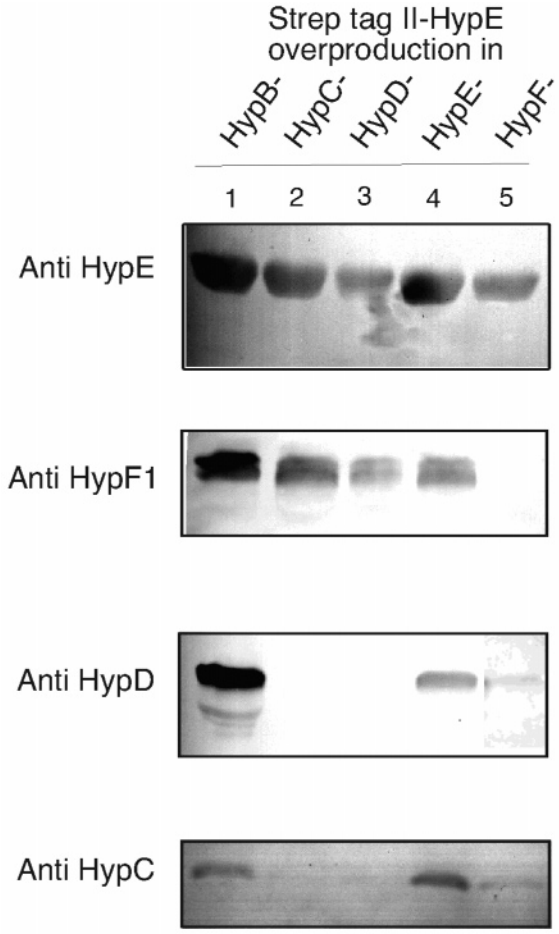

FIGURE 2: Immunoblot analysis of the Hyp proteins copurified with N-terminally *Strep*-tagged HypE in the *hyp* deletion strains. For detection using anti-HypD, -HypE, or -HypF1 sera, proteins were separated on 12% SDS−PAGE gels. For detection using anti-HypC serum, the proteins were separated on a 15% SDS−PAGE. Each lane contains 15 μL of protein from the third elution fraction of a *Strep*-tag affinity purification using cells of the indicated strain: lane 1, HF417[*hypB1*,*B2*Δ](p*hypE*$_{SN}$); lane 2, HF340[*hypC*Δ](p*hypE*$_{SN}$); lane 3, HF338[*hypD*Δ](p*hypE*$_{SN}$); lane 4, HF339[*hypE*Δ](p*hypE*$_{SN}$); lane 5, HF441[*hypF1*,*F2*Δ](p*hypE*$_{SN}$).

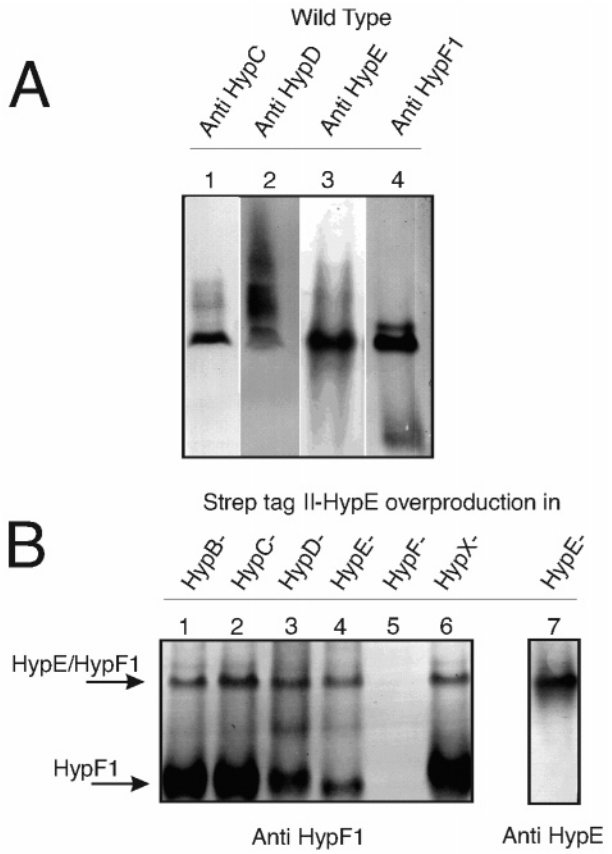

FIGURE 3: Immunoblot analysis of complexes of HypE. Proteins were separated on a 4−15% nondenaturing polyacrylamide gel. In panel A, samples were purified from HF339[*hypE*Δ](p*hypE*$_{SN}$) using the *Strep*-tag II affinity purification. The Western blot was then developed with the protein-specific antibody indicated at the top of the lane. Protein quantities are as follows: lane 1, 1 μg; lane 2, 5 μg; lane 3, 1 μg; lane 4, 5 μg. In panel B, samples were purified from the strains indicated at the top of each lane, and proteins were detected with specific antisera indicated at the bottom. Lanes 1−6 contain 5 μg of protein, and lane 7 contains 1 μg.

different categories of mutants can be identified. First, there are those mutants where all of HypC, HypD, and HypF1 copurified with HypE. This category includes HF339[*hypE*Δ](p*hypE*$_{SN}$) (effectively wild-type) and HF417(p*hypE*$_{SN}$), in which *hypB1* and *hypB2* were deleted. Second, there are those mutants in which only HypF1 and HypE were copurified, whereas HypC and HypD were not detected in the purified protein. HF338(p*hypE*$_{SN}$), which is *hypD*Δ, and HF340(p*hypE*$_{SN}$), which is *hypC*Δ, fall into this second category. Finally, HF441(p*hypE*$_{SN}$), which lacks both HypF1 and HypF2, forms a third category in which only traces of HypC and HypD were copurified with HypE. Thus it can be concluded that whenever both HypE and HypF1 were present these two proteins copuried. Furthermore, HypC and HypD copurified with HypE as a unit, that is, one was never observed without the other. Finally, their interaction with HypE was significantly destabilized by deletion of *hypF1* and *hypF2*.

Detection of HypE-Containing Complexes Using Nondenaturing Polyacrylamide Gels. As shown above, under wild-type conditions, N-terminally *Strep*-tagged HypE copurifies with HypC, HypD, and HypF1. This result could arise from several situations. For example, there could exist one large complex between HypC, HypD, HypE, and HypF1, or there may be several different complexes each including HypE and some subset of the other Hyp proteins. To establish whether multiple complexes were present in the purified samples, the eluted proteins were analyzed on 4−15% polyacrylamide-gradient, nondenaturing gels, as well as gels of different fixed percentages of acrylamide. Two methods were used to establish the molecular masses of complexes in native gels: estimation by comparison to a native protein standard, and electrophoresis on native gels having various percentages of acrylamide (see Materials and Methods for details). While the former method does not account for effects due to protein charge leading to errors in estimates of the masses of large complexes, the latter technique has significant errors for small molecular weight proteins (30−60 kDa) and can, at best, be considered appropriate for proteins in the range 40−500 kDa (*44*, *45*). Figure 3A shows that a spot at approximately the same height can be observed when a nondenaturing gel is blotted and analyzed with specific anti-HypC, -HypD, -HypE, or -HypF1 sera. By comparison with a native protein standard, it was estimated that the molecular masses of proteins migrating in this part of the gel were approximately 80 kDa. However, closer examination revealed that the exact heights of all of the bands

Table 2: Predicted Molecular Masses of Proteins and Protein Complexes Relevant to This Study

protein or complex	expected molecular mass (kDa)
HypC	9.8
HypD	41.9
HypE	36.6
HypF1	40.7
HoxH	54.9
HypC/HypD	51.7
HypC/HoxH	64.7
$(HypE)_2$	73.2
HypE/HypF1	77.3
HypC/HypD/HypE	88.4

were not obviously identical, making it impossible to say whether one or more complexes were present. On gradient native gels, the HypC-, HypD-, and HypE-specific signals began with a reasonably resolved band in the 80 kDa region and then proceed into a more smeared signal until approximately the 150 kDa region of the gel. This may indicate a range of complexes involving these proteins. By analysis of migration behavior on gels of various acrylamide concentrations, the fastest migrating complex was determined to have a molecular mass of approximately 70 kDa and the slowest a molecular weight of 152 kDa. Careful evaluation of the HypF1-specific signals showed that they consisted of three bands. The fastest running band corresponded to HypF1 alone and arose from HypF1 dissociating from complexes after purification or during electrophoresis. There were also two slower migrating signals at approximately the same position as the HypE-, HypC-, and HypD-specific signals. These two signals consisted predominantly of a faster migrating band and a significantly less intense but only slightly slower migrating band. Although this marginally slower HypF1 band was always less significant than the faster migrating form, the absolute amount of the slower migrating form varied considerably between different purification attempts. In some cases, it was quite obviously present and in others virtually undetectable. The origin of this variation is not yet clear.

Assuming a 1:1:1 stoichiometry, a HypC/HypD/HypE complex would have a molecular mass of 88.4 kDa and a 1:1 complex of HypE and HypF1 would have a molecular mass of 77.3 kDa (see Table 2 for a summary of predicted molecular masses relevant to this study). Thus it is possible that these complexes could migrate to similar positions in a nondenaturing gradient polyacrylamide gel, yielding results such as those presented in Figure 3.

Analysis of the HypE-containing complexes purified from other genetic backgrounds helped to clarify the situation. Figure 3B shows a Western blot analyzed using HypF1-specific antiserum and a lane detected with HypE-specific antiserum for comparison. The same pattern of HypF1 signals as described above was detected. The fastest running band corresponded to HypF1 alone and arises from HypF1 dissociating from complexes after purification or during the electrophoresis. The slower running band cross-reacts with the HypE-specific antibody suggesting that it is a HypE/HypF1 complex. Furthermore, the expected molecular mass of a 1:1 complex of HypE and HypF1, 77.3 kDa, corresponds well to an estimate of the molecular mass of this observed complex obtained by comparison to a native protein standard (80 kDa), as well as the molecular mass calculated from gels of various polyacrylamide concentrations (70 kDa). We note that there is no signal for HypE monomer arising from the dissociation of the HypE/HypF complex, lane 7, although there is a signal for the HypF1 monomer. The reason is that the stable form of HypE alone is a dimer, which runs to the same position on the native gel as the HypE/HypF1 complex (see results of HypE purification from HF210(p*hypE*$_{NS}$) presented below). Therefore, dissociation of this complex results in no new HypE-specific signal. The presence of this HypE/HypF1 complex did not depend on HypB, HypC, HypD, or HypX (see Figure 3), meaning that formation of this complex does not require other Hyp proteins.

HypE/HypF1 Complex Formation in Vitro. Copurification of HypC, HypD, and HypF1 with HypE suggests that these four proteins may form a large intermediate complex. This hypothesis is bolstered by the fact that only one obvious species was observed when this mixture was analyzed on a nondenaturing gel. On the other hand, the results presented in Figure 3 from the purification of HypE from HF338-[*hypC*Δ](p*hypE*$_{SN}$) and HF340[*hypD*Δ](p*hypE*$_{SN}$) implied that HypE and HypF1 alone were also capable of forming a complex even in the absence of HypC and HypD. Furthermore, this complex migrated to the same position in native gels irrespective of the genetic background. To establish whether HypE and HypF1 alone form a stable complex and where it migrates in the nondenaturing gel system, experiments were undertaken to prepare such a complex in vitro.

All of the hydrogenase-related genes in *R. eutropha* H16 are encoded on the megaplasmid pHG1 (*30*). Thus, to purify HypE and HypF without contamination from any other hydrogenase-related proteins, plasmids p*hypE*$_{SN}$ and p*hypF1*$_{SC}$ were introduced into HF210, a megaplasmid-free *R. eutropha* strain. HypE from HF210(p*hypE*$_{SN}$) and HypF1 from HF210-(p*hypF1*$_{SC}$) were purified using the *Strep*-tag affinity purification. The purified proteins were then mixed and incubated at room temperature for 10 minutes before application to a 4−15% nondenaturing polyacrylamide gel. Figure 4 shows the results of immunoblot analysis with anti-HypF1 and anti-HypE sera. First, lane 2 shows that HypF1 purified from HF210, that is, not copurified with any other hydrogenase-related proteins, yielded a single, faster-migrating band in the Western blot corresponding to HypF1 monomer. When this protein was mixed with HypE in vitro, a new slower-migrating band was observed (lane 3). In actuality, close inspection reveals that two new bands at approximately the same position were observed. This double band phenomenon was also observed in purified in vivo prepared HypE/HypF1 samples as discussed in the previous section (see also Figure 3). The relative amounts of these two new bands depended on the [HypE]/[HypF1] ratio with more of the slower migrating form present when higher concentrations of HypF1 were present (data not shown). These results show that two new forms of HypF1 could be produced in vivo by mixing with HypE. This result could arise from two situations: first, if HypE were able to modify HypF1 so that it migrated differently in the native gel system, perhaps as a dimer instead of a monomer; the second possibility is that HypE formed a complex with HypF1. Comparison of the position of the new HypF1 band with the position of the HypE/HypF1 band observed for in vivo complex purified from Hyp339-

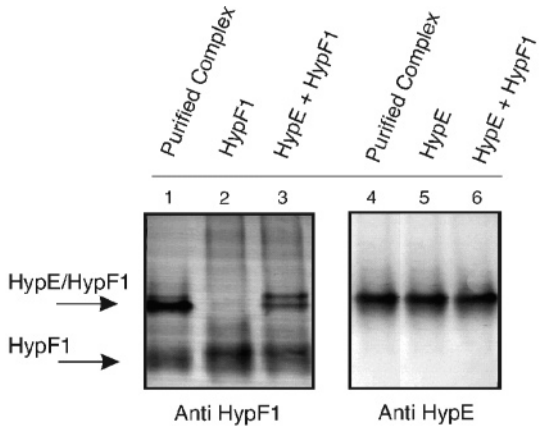

FIGURE 4: Immunolot analysis of complexes of HypF1 purified from cells or prepared in vitro. Proteins were separated on a 4−15% nondenaturing acrylamide gel and then detected with anti-HypF1 or anti-HypE serum: lane 1, 7.5 μg of the third elution fraction of a *Strep*-tag affinity purification of HF339[*hypE*Δ](p*hypE*$_{SN}$); lane 2, 1 μg of HypF1 purified from HF210(p*hypF1*$_{SC}$); lane 3, 2 μg of an equimolar mixture of HypF1 purified from HF210(p*hypF1*$_{SC}$) and HypE purified from HF210(p*hypE*$_{SN}$); lane 4, 1 μg of the third elution fraction of a *Strep*-tag affinity purification of HF339[*hypE*Δ]-(p*hypE*$_{SN}$); lane 5, 1 μg of the third elution fraction of a *Strep*-tag affinity purification of HF210(p*hypE*$_{SN}$); lane 6, 2 μg of an equimolar mixture of HypF1 purified from HF210(p*hypF1*$_{SC}$) and HypE purified from HF210(p*hypE*$_{SN}$).

[*hypE*Δ](p*HypE*$_{SN}$) cells (lane 1) showed that the two bands were in the same place, suggesting that at least one of the two new HypF1 forms prepared in vitro also arose from a HypE/HypF1 complex. In addition, immunoblot analysis with anti-HypE serum showed that this band also contained HypE (lanes 4 and 6). Therefore, the new HypF1 species created by adding HypE in vitro not only relied on HypE for formation but was a complex between HypE and HypF1. Furthermore, this complex was the same as the in vivo complex obtained by copurification of the Hyp proteins. We note that HypE alone, that is, purified from HF210 so that no other Hyp proteins are copurified, migrates to the same position in native gels as the HypE/HypF1 complex (lane 5). This suggests that HypE is stable as a dimer.

Purification of HypC. Since it was not clear in which complex or complexes HypC and HypD copurify with HypE, experiments were undertaken to purify Hyp protein complexes using the *Strep*-tag affinity procedure with the tag in other locations. Figure 5 shows a Coomassie-stained gel of the proteins resulting from the purification of HypC modified with a C-terminal *Strep*-tag from the strain HF340(p*hypC*$_{SC}$), in which *hypC* has been deleted. In addition to the non-hydrogenase-related contaminants also observed in the purification of HypE, there are two bands visible at the masses expected for HypD, HypE, or HypF1, as well as some strong bands in the region expected for HoxH (55 kDa), the NiFe-containing subunit of the SH. Western blot analysis identified the two bands running between 47.5 and 32.5 kDa as arising from HypD and HypE, in addition to confirming that the higher molecular mass band arose from HoxH, a protein that did not copurify with HypE. Also, in contrast to the results of purification of HypE, HypF1 did not copurify with HypC (Figure 5B). The effect of deletion of *hypF1* and *hypF2* on purification of HypC was similar to that observed for purification of HypE. This means that, as shown in Figure 5B, purification of HypC from HF441(*hypF1,F2*Δ)[p*hypC*$_{SC}$]

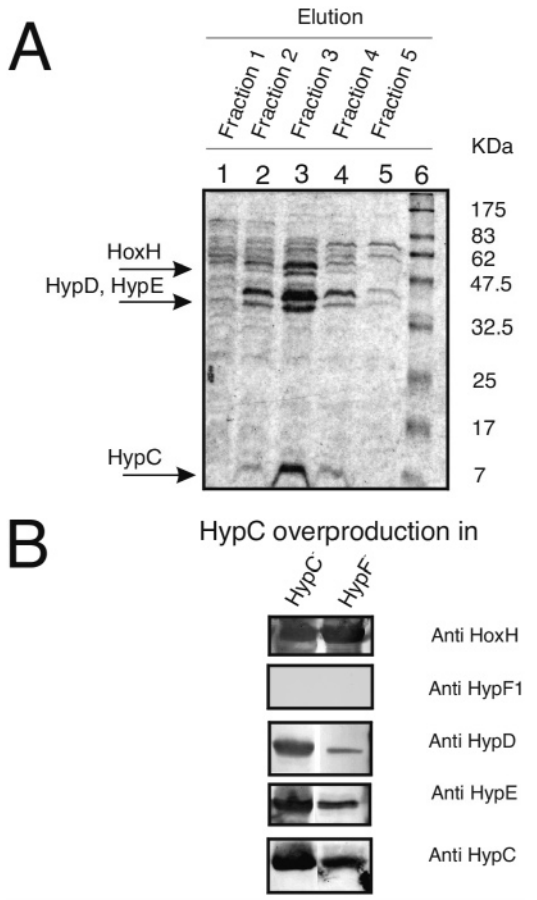

FIGURE 5: Purification of C-terminally *Strep*-tagged HypC from HF340[*hypC*Δ](p*hypC*$_{SC}$). In panel A, the indicated proteins were separated on a 15% SDS−PAGE gel and visualized with Coomassie brilliant blue: lane 1, first elution fraction; lane 2, second elution fraction; lane 3, third elution fraction; lane 4, fourth elution fraction; lane 5, fifth elution fraction; lane 6, standard proteins. From each elution fraction, 15 μL of solution was applied to the gel. Panel B shows Western blot analysis of the third elution fractions of the purification shown in panel A and the third elution fraction from a purification from HF441[hypF1Δ,hypF2Δ](p*hypC*$_{SC}$) using the specific antisera designated adjacently. Proteins were separated using a 12% SDS−PAGE for analysis with anti-HypD, anti-HypE, anti-HypF1, or anti-HoxH serum.

resulted in lesser amounts of copurified HypD and HypE, that is, deletion of *hypF* destabilized the interaction between HypC, HypD, and HypE.

To establish how many complexes were copurified, the purified proteins were again analyzed on various polyacrylamide, nondenaturing gels. Lanes 1 and 3 of Figure 6 show that the purified protein contained at least two, if not three, complexes involving HypC. The fastest running form clearly cross-reacted with anti-HoxH serum (lane 9) but not anti-HypD (lane 5) or -HypE (lane 7) serum. Its molecular mass, estimated by comparing migration with respect to a native protein standard, should be approximately 65 kDa. Calculation of the molecular mass using the method of Hederick and Smith leads to a value of 45 kDa. These estimates correspond well to the expected molecular mass of a 1:1 HoxH/HypC complex, 64.7 kDa. Taken together, these results strongly suggest that it was exclusively a complex between HypC and the large subunit of the SH, HoxH. The second, slower running form of HypC cross-reacted with anti-HypD serum but not with HoxH antiserum. This demonstrates that HypD but not HoxH was involved in this

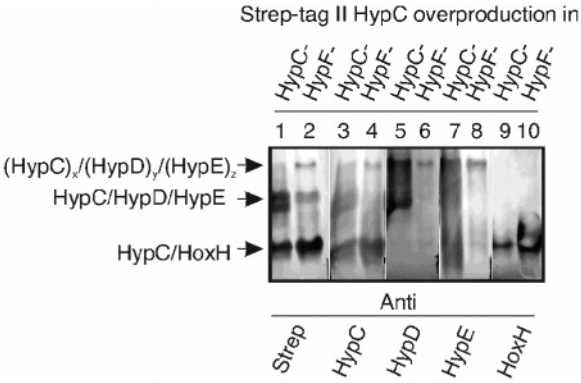

FIGURE 6: Immunoblot analysis of the complexes present in HypC purified from the strains listed at the top of each lane. HypC$^-$ is HF340[*hypC*Δ](p*hypC*$_{SC}$) and HypF$^-$ is HF441[*hypF1*,*F2*Δ]-(p*hypC*$_{SC}$). The subscripts *x*, *y*, and *z* refer to unknown protein stoichiometries in complexes. Proteins were separated on a 4−15% nondenaturing polyacrylamide gel. The Western blots were then developed with the protein-specific antibody indicated at the bottom of each lane. Lanes developed using *Strep*-tag II specific antibody contain 5 μg of protein, those using HypC antibody 2 μg of protein, those using HypD antibody 10 μg of protein, those using HypE antibody 10 μg of protein, and those using HoxH 5 μg of protein.

complex. Whether HypE participates in this complex is unclear since the reaction with HypE-specific antibody is smeared in this region. Comparison with native protein standard suggested that complexes of molecular masses of approximately 80−100 kDa migrate to this part of the gel. Furthermore, the migratory behavior of this complex analyzed using the method of Hederick and Smith suggests that the complex has a molecular mass of 70 kDa. Thus, it is improbable that this is a 1:1 HypC/HypD complex. However, a 1:1:1 complex of HypC/HypD/HypE would have the expected molecular mass, 88.4 kDa. Finally, a third, slowest migrating form, reacted strongly with HypD- and HypE-specific antisera. Its molecular mass could be estimated to be approximately 150 kDa based on comparison to the native standard and 152 kDa using the method of Hederick and Smith. The reaction on this position of the gel with HypC- and *Strep*-tag-specific antisera can be described more as a smear than as a band. However, when HypC purified from the HypF$^-$ strain is considered (lanes 2, 4, 6, 8, and 10), it becomes clear that this slowest migrating form does react with both HypC and *Strep*-specific antibodies. Thus, it represents a complex between all of HypC, HypD, and HypE and seems to be stabilized in the absence of HypF. Given the high molecular mass of this complex, it should contain multiple copies of one or more of the Hyp proteins present. The HoxH/HypC complex is unaffected by the deletion of *hypF*, but the intermediately migrating forms of HypC were destabilized relative to the slowest migrating forms.

DISCUSSION

Hydrogenases catalyze one of the most fundamental chemical reactions, the splitting of hydrogen into protons and electrons. While fundamental, this reaction is by no means simple, and the biological architecture of hydrogenases is correspondingly complex. Posttranslational maturation of hydrogenases is a complicated process involving biosynthesis of the hydrogen-activating site, hydrogenase subunit oligomerization, and, in some cases, transport and insertion into a membrane. The biosynthesis of the active site alone is known to require the six conserved *hyp* genes, *hypA*−*F*. Despite the fact that these genes have been observed in many organisms, little work has been reported characterizing the functions of the gene products and thus the biochemistry of NiFe active site biosynthesis. A working model of NiFe active site biosynthesis has been developed using data almost exclusively derived from experiments with *E. coli* (*9*). This model suggests that using carbamoyl phosphate as a precursor the diatomic ligands are synthesized by HypE and HypF and then transferred to an Fe fragment housed in a HypC/HypD complex. The iron fragment shuttles with HypC from the HypC/HypD complex to a new complex with the immature large subunit. The synthesis is completed by Ni incorporation through the actions of HypA and HypB. *E. coli* produces hydrogenases exclusively under anaerobic conditions. There exist, on the other hand, organisms, such as *R. eutropha*, that produce hydrogenases only under aerobic conditions. In addition to the six conserved *hyp* genes, these organisms harbor another *hyp* gene, *hypX*, required for synthesis of fully active hydrogenases (*10*, *12*). Identifying and understanding differences in the aerobic versus anaerobic biosynthesis of NiFe hydrogenases may be a crucial step in developing hydrogenase-based biotechnological applications.

In this paper, we have begun to characterize the mechanism of NiFe active site biosynthesis in *R. eutropha* by identifying several complexes of the Hyp proteins formed in vivo. These complexes have been partially purified via affinity purification using a *Strep*-tag II sequence and their components characterized using immunological analysis. Attaching a *Strep*-tag II to the C-terminus of HypE leads to physiologically inactive protein. Reissmann and co-workers (*15*) have shown that the C-terminal cysteine of HypE from *E. coli* can be modified in the presence of carbamoyl phosphate, ATP, and HypF with a CN^- group. The inactivity of a *R. eutropha* HypE variant in which this cysteine is blocked by the *Strep*-tag II suggests that this mechanism may also operate in *R. eutropha*. When the *Strep*-tag is attached to the N-terminus of HypE, the protein regains physiological activity and can be copurified with HypC, HypD, and HypF1 (Figures 1 and 2). Under none of the conditions investigated did HypB, HypX, or HoxH copurify with HypE, suggesting that they do not form stable complexes with HypE.

Analysis of nondenaturing gels and purification of HypE from different genetic backgrounds helped to identify several distinct complexes involving HypE. First, whenever HypF1 is present, it copurifies with HypE (Figure 2). This HypE/HypF1 complex migrated to the same position in native gels irrespective of genetic background and could be reconstituted in vitro (Figures 3B and 4). This demonstrates that HypE and HypF1 form a stable complex that does not rely on any of the other Hyp proteins for formation. In fact, close examination suggests that two HypE/HypF1 complexes may be formed. The difference between these two forms must be subtle since they migrate to almost exactly the same position on native gels. Furthermore, it is clear that none of the other Hyp proteins are involved in these HypE/HypF1 complexes since they are formed in vitro using proteins purified from HF210, that is, not containing any other Hyp proteins. Thus the difference between the two complexes must correspond to a small chemical or conformational change. Attempts to establish the difference between these two forms are ongoing.

Scheme 1: Schematic Model of the Interactions between HypC, HypD, HypE, and HypF1 in *R. eutropha* Based on the Results of This Study[a]

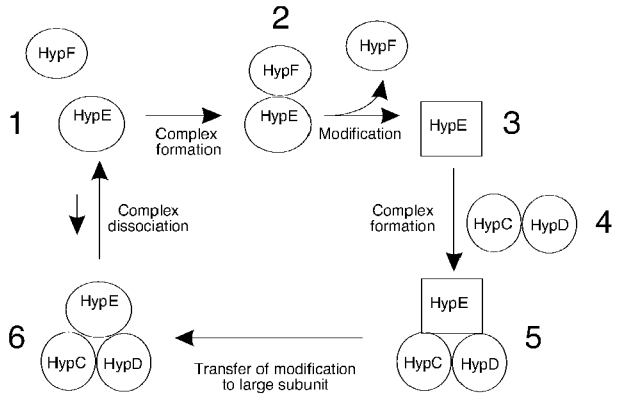

[a] The change in shape from a circle to a square of HypE indicates a change caused by HypF that allows interaction with the HypC/HypD complex to take place.

Under wild-type-like conditions, HypC and HypD also copurify with HypE. However, when HypF1 and HypF2 are absent, HypE copurifies with only trace amounts of HypC and HypD. Furthermore, if either HypC or HypD is absent, then the other is not able to copurify with HypE. These results suggest that HypC and HypD can interact with HypE only as a complex and that this HypC/HypD has an increased affinity for HypE after it has been modified in some way by the action of HypF. This scheme of events is depicted as complexes 1−5 in Scheme 1. The HypC/HypD/HypE complex purified using a *Strep*-tag on HypE must primarily be complex 5 of Scheme 1 as opposed to complex 6 since HypE purified from HF339[*hypE*Δ](p*hypE*$_{SN}$) contained easily detectable amounts of HypC and HypD, whereas HypE purified from HF441[*hypF1*Δ,*hypF2*Δ](p*hypE*$_{SN}$) contained only trace amounts of HypC and HypD. The precise stoichiometry of this HypC/HypD/HypE complex is difficult for two reasons to estimate. First, HypD and HypE have similar molecular masses, and second, native gel analysis suggests a range of complexes with molecular masses between 80 and 150 kDa may be formed. This suggests that the smallest complex is most likely a 1:1:1 complex, while the largest may involve single copies of HypC and HypD bound to a trimer of HypE. This observed range of HypC/HypD/HypE complexes may be physiologically relevant to hydrogenase maturation since exactly three ligands, one CO and two CN^-, must be incorporated into the immature hydrogenase large subunit. It is possible that all three ligands are delivered simultaneously from a large HypC/HypD/HypE complex to the immature hydrogenase large subunit.

Purification of *Strep*-tagged HypC provided additional circumstantial evidence that no stable HypC/HypD/HypE/HypF1 complex forms since HypF1 is never copurified while purifying HypC. Furthermore, evidence for the HypC/HypD/HypE complex depicted as complex 6 is obtained from the purification of HypC from HF441[*hypF1*Δ,*hypF2*Δ](p*hypC*$_{SC}$) (Figure 6). The deletion of HypF means that HypE is no longer able to interact with HypF. Therefore, the driving force for the decomposition of the complex between HypC and HypD and unmodified HypE is decreased, and this HypC/HypD/HypE complex, complex 6, becomes more readily observable as the prominent, slowest migrating protein complex. Since *E. coli* HypF is able to modify the C-terminus of HypE with a CN^- (*15*) and, as shown above, *R. eutropha* HypE is inactive with a *Strep*-tag on the C-terminus, we hypothesize that the HypF-dependent modification required for strong interaction of HypE with HypC/HypD in *R. eutropha* is the incorporation of a diatomic ligand at the C-terminus of HypE. To create active hydrogenase, this diatomic ligand must be transferred from HypE to the immature hydrogenase large subunit. We suggest that this transfer takes place from the HypC/HypD/HypE complex 5 and generates as product complex 6. The need for the activated HypC/HypD/HypE complex, complex 5, to interact with other proteins may explain its relative stability. As a maturation intermediate, it might be expected to be only transiently formed. The details of the supposed ligand transfer process remain to be elucidated, and spectroscopic analysis of the two HypC/HypD/HypE complexes is underway.

The purifications of HypC from different genetic backgrounds also shed light on the actions of HypC in *R. eutropha*. To provide a more general picture of NiFe site biosynthesis, the results presented here using *R. eutropha* proteins must be compared with what is already known from *E. coli*. In a study of an *E. coli* Δ*carAB* mutant by Blokesch and Böck (*16*), that is, a mutant blocked in carbamoyl phosphate synthetase, a HypC/HypD complex was identified. This HypC/HypD complex was resolved upon addition of citrulline, an indirect carbamoyl phosphate source, with concomitant appearance of a HypC/HycE complex, where HycE is the large subunit of hydrogenase 3 in *E. coli*. The authors then suggested that HypC participates in a cycle performing a transfer function, that is, that HypC with the Fe and diatomic ligands is transferred from HypD to the immature large subunit.

The proposed mechanism of HypC shuttling between HypC/HypD complex and HypC/large subunit complex appears not to operate in *R. eutropha* since HypC/HoxH complex was purified in significant quantities from strains containing p*hypC*$_{SC}$ and deleted for *hypB* (HF417(p*hypC*$_{SC}$)), *hypE* (ypEHF339(p*hypC*$_{SC}$)), and *hypF* (HF441(p*hypC*$_{SC}$)) (data for HF417 and HF339 not shown). If we assume that HypE and HypF are essential for diatomic ligand synthesis in *R. eutropha*, then it appears that diatomic ligand synthesis is not crucial for HypC/HoxH complex formation. This result is more in keeping with the ideas of Maróti and co-workers (*47*) who suggested that two HypC-like proteins are needed for each HypC cycle, that is, one for interacting with HypD and one for interacting with hydrogenase large subunit, with the two functions having no intrinsic link. In *R. eutropha*, it seems that the two functions, that is, chaperoning HoxH and functioning in $Fe(CO)(CN)_2$ synthesis in a complex with HypD, are not linked, that is, one does not necessarily require or follow the other in the maturation pathway. Rather the two functions seem to take place in parallel. However, at least with respect to SH maturation, the two functions do not appear to be separated between two HypC-like proteins; the same protein, HypC, performs both functions.

It is perhaps surprising that HypF1 copurifies with HypE. *R. eutropha* codes for two different HypF proteins assigned to the genes *hypF1* and *hypF2*, respectively. HypF2 is a standard HypF containing the three strongly conserved sequence motifs: an N-terminal acyl phosphatase motif, two perfect zinc finger motifs, and a C-terminal motif containing

three conserved histidines thought to be involved in interaction with carbamoyl phosphate (*14*, *32*). HypF1, however, is a truncated protein containing only the C-terminal motif. Paschos and co-workers (*14*) have demonstrated for *E. coli hypF* that mutations in any of these three motifs lead to inactive protein. On the other hand, *hyp* mutants prepared in *R. eutropha* show that HypF1 and HypF2 are both active in the production of hydrogenases. The results of this study, that is, the copurification of HypE and HypF1, provide additional evidence that HypF1 plays a role in hydrogenase maturation in *R. eutropha*. At the very least, HypE is able to form a stable complex with HypF1 both in vivo and in vitro. It remains a possibility that this complex does not contain all of the functions necessary for diatomic ligand synthesis but requires another component for complete activity. Experiments are now underway to characterize the in vitro activity of purified HypF1.

Having successfully purified several hydrogenase maturation intermediates, it is now possible to consider biochemical characterization of these complexes in vitro especially using FTIR spectroscopy, a technique that can be used to detect the presence of Fe-bound CO and CN^-. Particular targets for such studies include the HypC/HypD/HypE and HoxH/HypC complexes. Such studies may help to clarify the mechanism of the biosynthesis of the biologically unusual hydrogenase diatomic ligands.

ACKNOWLEDGMENT

T. Burgdorf is thanked for helpful discussions. E. Krause is acknowledged for completing mass spectrometry experiments. J. Stöhr is thanked for excellent technical assistance.

REFERENCES

1. Cammack, R. (2001) Hydrogenases and their activities, in *Hydrogen as a Fuel* (Cammack, R., Frey, M. and Robson, R., Eds.) pp 73−92, Taylor & Francis, London.
2. Bagley, K. A., Duin, E. C., Roseboom, W., Albracht, S. P. J., and Woodruff, W. H. (1995) Infrared-detectable groups sense changes in charge density on the nickel center in hydrogenase from *Chromatium vinosum*, *Biochemistry 34*, 5527−5535.
3. Nicolet, Y., Piras, C., Legrand, P., Hatchikian, C. E., and Fontecilla-Camps, J. C. (1999) *Desulfovibrio desulfuricans* iron hydrogenase: the structure shows unusual coordination to an active site Fe binuclear center, *Struct. Fold. Des. 7*, 13−23.
4. Nicolet Y., Lemon B. J., Fontecilla-Camps J. C., and Peters J. W. (2000) A novel FeS cluster in Fe-only hydrogenases, *Trends Biochem. Sci*. *25*, 138−143.
5. Peters, J. W., Lanzilotta, W. N., Lemon, B. J., and Seefeldt, L. C. (1998) X-ray crystal structure of the Fe-only hydrogenase (CpI) from *Clostridium pasteurianum* to 1.8 angstrom resolution, *Science 282*, 1853−1858.
6. Volbeda, A., Charon, M. H., Piras, C., Hatchikian, E. C., Frey, M., and Fontecilla-Camps, J. C. (1995) Crystal structure of the nickel−iron hydrogenase from *Desulfovibrio gigas*, *Nature 373*, 580−587.
7. Volbeda, A., Garcin, E., Piras, C., De Lacey, A., Fernandez, V. M., Hatchikian, E. C., Frey, M., and Fontecilla-Camps, J. C. (1996) Structure of the [NiFe] hydrogenase active site: Evidence for biologically uncommon Fe ligands, *J. Am. Chem. Soc. 118*, 12989−12996.
8. Vignais, P. M., Billoud, B., and Meyer, J. (2001) Classification and phylogeny of hydrogenases, *FEMS Microbiol. Rev. 45*, 455−501.
9. Blokesch, M., Paschos, A., Theodoratou, E., Bauer, A., Hube, M., Huth, S., and Böck, A. (2002) Metal insertion into proteins, *Biochem. Soc. Trans. 30*, 674−680.
10. Buhrke, T., and Friedrich, B. (1998) *hoxX* (*hypX*) is a functional member of the *Alcaligenes eutrophus hyp* gene cluster, *Arch. Microbiol. 170*, 460−463.
11. Durmowicz, M. C., and Maier, R. J. (1997) Roles of HoxX and HoxA in biosynthesis of hydrogenase in *Bradyrhizobium japonicum*, *J. Bacteriol*. *179*, 3676−3682.
12. Rey, L., Fernandez, D., Brito, B., Hernando, Y., Palacios, J. M., Imperial, J., and Ruiz-Argueso, T. (1996) The hydrogenase gene cluster of *Rhizobium leguminosarum bv. viciae* contains an additional gene (*hypX*), which encodes a protein with sequence similarity to the N_{10}-formyltetrahydrofolate-dependent enzyme family and is required for nickel-dependent hydrogenase processing and activity, *Mol. Gen. Genet. 252*, 237−248.
13. Paschos, A., Glass, R. S., and Böck, A. (2001) Carbamoyl phosphate requirement for synthesis of the active center of [NiFe]-hydrogenases, *FEBS Lett. 488*, 9−12.
14. Paschos, A., Bauer, A., Zimmermann, A., Zehelein, E. and Böck, A. (2002) HypF, a carbamoyl phosphate converting enzyme involved in [NiFe] hydrogenase maturation, *J. Biol. Chem. 277*, 49945−49951.
15. Reissmann, S., Hochleitner, E., Wang, H., Paschos, A., Lottspeich, F., Glass, R. S., and Böck, A. (2003) Taming of a Poison: Biosynthesis of the NiFe-hydrogenase cyanide ligands, *Science 299*, 1067−1070.
16. Blokesch, M., and Böck, A. (2002) Maturation of [NiFe]-hydrogenases in *Escherichia coli*. The HypC cycle, *J. Mol. Biol. 324*, 287−296.
17. Drapal, N., and Böck, A. (1998) Interaction of the hydrogenase accessory protein HypC with HycE, the large subunit of *Escherichia coli* hydrogenase 3 during enzyme maturation, *Biochemistry 37*, 2941−2948.
18. Fodor, B. D., Kovács, A. T., Csáki, R., Hunyadi-Gulyás, E., Klement, E., Maróti, G., Mészáros, L. S., Medzihradszky, K. F., Rákhely, G., and Kovács, K. L. (2004) Modular broad-host range expression vectors for single-protein and protein complex purification, *Appl. Environ. Microbiol. 70*, 712−721.
19. Magalon, A. and Böck, A. (2000) Analysis of the HypC−HycE complex, a key intermediate in the assembly of the metal center of the *Escherichia coli* hydrogenase 3, *J. Biol. Chem. 275*, 21114−21220.
20. Maier, T., Lottspeich, and Böck, A. (1995) GTP hydrolysis by HypB is essential for nickel insertion into hydrogenases of *Escherichia coli*, *Eur. J. Biochem. 230*, 133−138.
21. Olson, J. W., Mehta, N. S., and Maier, R. J. (2001) Requirement of nickel metabolism proteins HypA and HypB for full activity of both hydrogenase and urease in *Helicobacter pylori*, *Mol. Microbiol. 39*, 176−182.
22. Fritsche, E., Paschos, A., Beisel, H. G., Böck, A., and Huber, R. (1999) Crystal structure of the hydrogenase maturating endopeptidase HybD from *Escherichia coli*, *J. Mol. Biol. 288*, 989−998.
23. Thiemermann, S., Dernedde, J., Bernhard, M., Schröder, W., Massanz, C., and Friedrich, B. (1996) Carboxy-terminal processing of the soluble, NAD-reducing hydrogenase of *Alcaligenes eutrophus* requires the *hoxW* gene product, *J. Bacteriol. 178*, 2368−2374.
24. Theodoratou, E., Paschos, A., Mintz-Weber, S., and Böck, A. (2000) Analysis of the cleavage site specificity of the endopeptidase involved in the maturation of the large subunit of hydrogenase 3 from *Escherichia coli*, *Arch. Microbiol. 173*, 110−116.
25. Theodoratou, E., Paschos, A., Magalon, A., Fritsche, E., Huber, R., and Böck, A. (2000) Nickel serves as a substrate recognition motif for the endopeptidase involved in hydrogenase maturation, *Eur. J. Biochem. 267*, 1995−1999.
26. Kleihues, L., Lenz, O., Bernhard, M., Buhrke, T., and Friedrich, B. (2000) The H_2 sensor of *Ralstonia eutropha* is a member of the subclass of regulatory [NiFe] hydrogenases, *J. Bacteriol. 182*, 2716−2724.
27. Schink, B., and Schlegel, H. G. (1979) The membrane-bound hydrogenase of *Alcaligenes eutrophus*. I. Solubilization, purification, and biochemical properties, *Biochim. Biophys. Acta 567*, 315−324.
28. Schneider, K., and Schlegel, H. G. (1976) Purification and properties of the soluble hydrogenase from *Alcaligenes eutrophus* H16, *Biochim. Biophys. Acta 452*, 66−80.
29. Happe, R. P., Roseboom, W., Egert, G., Friedrich, C. G., Massanz, C., Friedrich, B., and Albracht, S. P. J. (2000) Unusual FTIR and EPR properties of the H_2-activating site of the cytoplasmic NAD-reducing hydrogenase from *Ralstonia eutropha*, *FEBS Lett. 466*, 259−263.
30. Schwartz, E., Henne, A., Cramm, R., Eitinger, T., Friedrich, B., and Gottschalk, G. (2003) Complete nucleotide sequence of

pHG1: A *Ralstonia eutropha* H16 megaplasmid encoding key enzymes of H_2-based lithoautotrophy and anaerobiosis, *J. Mol. Biol. 332*, 369−383.
31. Dernedde, J., Eitinger, T., Patenge, N., and Friedrich, B. (1996) *hyp* gene products in *Alcaligenes eutrophus* are part of a hydrogenase maturation system, *Eur. J. Biochem. 235*, 351−358.
32. Wolf, I., Buhrke, T., Dernedde, J., Pohlmann, A., and Friedrich, B. (1998) Duplication of the *hyp* genes involved in maturation of [NiFe] hydrogenases in *Alcaligenes eutrophus* H16, *Arch. Microbiol. 170*, 451−459.
33. Yanisch-Perron, C., Vieira, J., and Messing, J. (1985) Improved M13 phage cloning vectors and host strains: nucleotide sequences of the M13mp18 and pUC19 vectors, *Gene 33*, 103−119.
34. Simon, R., Priefer, U., and Pühler, A. (1983) A broad host range mobilization system for in vivo genetic engineering: transposon mutagenesis in gram-negative bacteria, *Bio/Technology 1*, 717−743.
35. Priefert, H., Hein, S., Krüger, N., Zeh, K., Schmidt, B., and Steinbüchel, A. (1991) Identification and molecular characterization of the *Alcaligenes eutrophus* H16 *aco* operon genes involved in acetoin catabolism, *J. Bacteriol. 173*, 4056−4071.
36. Srivastava, S., Urban, M., and Friedrich, B. (1982) Mutagenesis of *Alcaligenes eutrophus* by insertion of the drug-resistance transposon Tn5, *Arch. Microbiol. 131*, 203−207.
37. Marx, C. J., and Lindstrom, M. E. (2001) Development of improved versatile broad-host range vectors for use in methylotrophs and other gram-negative bacteria, *Microbiology 147*, 2065−2075.
38. Eberz, G., Hogrefe, C., Kortlüke, C., Kamienski, A., and Friedrich, B. (1986) Molecular cloning of structural and regulatory hydrogenase (*hox*) genes of *Alcaligenes eutrophus* H16, *J. Bacteriol. 168*, 636−641.
39. Schwartz, E., Gerischer, U., and Friedrich, B. (1998) Transcriptional regulation of *Alcaligenes eutrophus* hydrogenase genes, *J. Bacteriol. 180*, 3197−3204.
40. Bradford, M. M. (1976) A rapid sensitive method for the quantitation of microgram quantities of protein utilizing the principle of protein-dye binding, *Anal. Biochem. 72*, 248−254.
41. Schneider, K., and Piechulla, B. (1986) Isolation and immunological characterization of the four nonidentical subunits of the soluble NAD-linked hydrogenase from Alcaligenes eutrophus H16, *Biochimie 68*, 5−13.
42. Lämmli, U. K. (1970) Cleavage of structural proteins during the assembly of the head of bacteriophage T4, *Nature 227*, 680−685.
43. Towbin, H., Staihelin, T., and Gordon, J. (1979) Electrophoretic transfer of protein from polyacrylamide gels to nitrocellulose sheets: procedure and some applications, *Proc. Natl. Acad. Sci. U.S.A.* 76, 4350−4354.
44. Spinelli, S., Fiérobe, H.-P., Belaïch, A., Belaïch, J.-P., Henrissat, B., and Cambillau, C. (2000) Crystal structure of a cohesion module from Clostridium cellulolyticun: Implications for dockerin recognition, *J. Mol. Biol. 304*, 189−200.
45. Hedrick, J. L., and Smith, A. J. (1968) Size and charge isomer separation and estimation of molecular weights of proteins by disc gel electrophoresis, *Arch. Biochem. Biophys. 126*, 155−164.
46. Buhrke, T., Bleijlevens, B., Albracht, S. P. J., and Friedrich, B. (2001) Involvement of *hyp* gene products in maturation of the H_2-sensing [NiFe] hydrogenase of *Ralstonia eutropha*, *J. Bacteriol. 183*, 7087−7093.
47. Maróti, G., Fodor, B. D., Rákhely, G., Kovács, A. T., Arvani, S., and Kovács, K. L. (2003) Accesory proteins functioning selectively and pleiotropically in the biosynthesis of the [NiFe] hydrogenase in *Thiocapsa roseopersicina*, *Eur. J. Biochem. 270*, 2218−2227.

BI048837K